Journal of Pharmaceutical Sciences 107 (2018) 2160-2171

Contents lists available at ScienceDirect

Journal of Pharmaceutical Sciences

journal homepage: www.jpharmsci.org

Pharmaceutics, Drug Delivery and Pharmaceutical Technology

Formulation Development, Optimization, and *In Vitro—In Vivo* Characterization of Natamycin-Loaded PEGylated Nano-Lipid Carriers for Ocular Applications

Akash Patil [1], Prit Lakhani [1], Pranjal Taskar [1], Kai-Wei Wu [1], Corinne Sweeney [1], Bharathi Avula [2], Yan-Hong Wang [2], Ikhlas A. Khan [2,3], Soumyajit Majumdar [1,*]

[1] *Department of Pharmaceutics and Drug Delivery, School of Pharmacy, University of Mississippi, Oxford, Mississippi 38677*
[2] *National Center for Natural Products Research, Research Institute of Pharmaceutical Sciences, University of Mississippi, Oxford, Mississippi 38677*
[3] *Division of Pharmacognosy, Department of BioMolecular Sciences, School of Pharmacy, University of Mississippi, Oxford, Mississippi 38677*

ARTICLE INFO

Article history:
Received 7 December 2017
Revised 12 February 2018
Accepted 17 April 2018
Available online 24 April 2018

Keywords:
ophthalmic drug delivery
antiinfective(s)
liposome(s)
pegylation
in vitro/in vivo (IVIVC) correlation(s)
bioavailability

ABSTRACT

The present study aimed at formulating and optimizing natamycin (NT)-loaded polyethylene glycosylated nano-lipid carriers (NT-PEG-NLCs) using Box-Behnken design and investigating their potential in ocular applications. Response surface methodology computations and plots for optimization were performed using Design-Expert® software to obtain optimum values for response variables based on the criteria of desirability. Optimized NT-PEG-NLCs had predicted values for the dependent variables which are not significantly different from the experimental values. NT-PEG-NLCs were characterized for their physicochemical parameters; NT's rate of permeation and flux across rabbit cornea was evaluated, *in vitro*, and ocular tissue distribution was assessed in rabbits, *in vivo*. NT-PEG-NLCs were found to have optimum particle size (<300 nm), narrow polydispersity index, and high NT entrapment and NT content. *In vitro* transcorneal permeability and flux of NT from NT-PEG-NLCs was significantly higher than that of Natacyn®. NT-PEG-NLC (0.3%) showed improved delivery of NT across the intact cornea and provided concentrations statistically similar to the marketed suspension (5%) in inner ocular tissues, *in vivo*, indicating that it could be a potential alternative to the conventional suspension during the course of fungal keratitis therapy.

Introduction

Fungal infections of the eye are serious clinical concerns and can lead to vision loss.[1-4] According to an analysis by Collier et al.[2] in *Morbidity and Mortality Weekly Report* for Centers for Disease Control and Prevention, incidence rates for keratitis were the highest amongst all the ocular infections, with an estimated 930,000 visits to doctor's office and outpatient clinics and about 58,000 emergency department visits annually with about 76.5% of keratitis visits requiring drug prescriptions. Episodes of keratitis and other ocular corneal infections approximated $175 million in direct health-care expenditures that included $58 million for Medicare patients and $12 million for Medicaid patients annually in the United States.

Natamycin (NT) has been one of the forerunners in ocular antifungal pharmacotherapy, especially in the management of fungal keratitis.[5] It has been used as a first-line antifungal agent because of its action against filamentous fungi causing ocular fungal infections (OFI) and better ocular safety/tolerability compared with the other antifungal agents.[6] However, one of the major challenges associated with NT is that intravenous and subconjunctival injections do not lead to therapeutic concentrations in the eye.[7] Upon topical application, NT shows low retention and a bioavailability (BA) of only 2%, necessitating frequent administration (initially given every hour/2 h and then tapered to 6-8 times a day).[8] In many cases, concomitant oral or systemic administration of NT or another antifungal agent, in addition to its topical application, is frequently required.[8] Although this coadministration provides good therapeutic outcomes, it is associated with the manifestation of ocular and systemic toxicities and an increase in the cost of therapy.

Conflicts of interest: The authors have declared no conflict of interests regarding this article.

* *Correspondence to:* Soumyajit Majumdar (Telephone: (662) 915-3793).
E-mail address: majumso@olemiss.edu (S. Majumdar).

https://doi.org/10.1016/j.xphs.2018.04.014
0022-3549/

Table 1
Independent Factors and Dependent Variables With Their Coded Levels of Box-Behnken Design

Factors	Coded Levels		
Independent factors	Level 1	Level 2	Level 3
A: Precirol® ATO 5 (mg)	150	300	450
B: castor oil (mg)	100	150	200
C: Span® 80 (mg)	0	20	40
D: HPH time (mins)	5	10	15
Dependent variables	Constraints		
Y_1: particle size	Optimum (<300 nm)		
Y_2: PDI	Minimum		
Y_3: % entrapment	Maximum		
Y_4: % DL	Maximum		

Currently, NT is the only commercially available topical agent (Natacyn® eye drops) used for the treatment of OFI. However, as previously mentioned, these eye drops are associated with 2 major challenges; the first being low retention and BA and the second being low penetration into the inner ocular tissues.[7,9] This necessitates the reformulation of NT as a different dosage form to harness its antifungal activity while overcoming the challenges associated with its delivery as eye drops.

In search of alternative strategies for the delivery of NT, nanolipid carriers (NLCs) were evaluated because they are known to enhance both BA and penetration of drugs into deeper tissues.[10-12] Surface-modified NLCs with polyethylene glycol (PEG-NLCs) have shown enhanced penetration, improved BA with lower toxicity profiles, and better stability upon storage in comparison to the normal NLCs.[13-17] This has been abundantly evidenced in the delivery of anticancer drugs in cancer chemotherapy. Therefore, in the present study, we sought to formulate and optimize NT-loaded PEGylated NLCs (NT-PEG-NLCs) using Box-Behnken design and evaluate and compare their efficacy with the marketed NT formulation (Natacyn®), *in vitro* and *in vivo*.

Table 2
Box-Behnken Design for the Experiment

Run	Precirol® ATO 5 (mg) (A)	Castor Oil (mg) (B)	Span® 80 (mg) (C)	HPH Time (mins) (D)
1	300	100	0	10
2	150	150	40	10
3	450	100	20	10
4	300	200	0	10
5	300	200	20	5
6	450	150	0	10
7	300	100	20	15
8	300	150	40	5
9	150	150	0	10
10	450	150	20	5
11	450	150	20	15
12	150	150	20	5
13	300	100	40	10
14	300	100	20	5
15	450	150	40	10
16	300	200	40	10
17	300	150	0	15
18	300	150	40	15
19	150	100	20	10
20	300	150	20	10
21	150	150	20	15
22	300	200	20	15
23	300	150	0	5
24	450	200	20	10
25	150	200	20	10

Materials and Methods

Chemicals

NT was purchased from Cayman Chemicals (Ann Arbor, MI). N-(carbonyl-methoxypolyethylenglycol-2000)-1,2-distearoyl-sn-glycero-3-phosphoethanolamine sodium salt (mPEG-2K-DSPE sodium salt) was purchased from Lipoid (Ludwigshafen, Germany). Precirol® ATO 5 was a generous gift from Gattefossé (Paramus, NJ). Castor oil, Tween® 80, Span® 80, poloxamer 188, and glycerin were all purchased from Acros Organics (Morris, NJ).

Methods

Screening of Lipid Excipients

NLCs are composed of solid and liquid lipids; hence, to select the most optimum solid and liquid lipids for the NT-PEG-NLCs, a lipid screening study was undertaken. Three solid lipids (Compritol® 888 ATO, Precirol® ATO 5, and glyceryl monostearate) and 9 liquid lipids (castor oil, olive oil, soybean oil, sesame oil, Maisine® CC, Labrafac® lipophile WL 1349, oleic acid, Miglyol® 829, and Captex® 355 EP) were screened. Briefly, 100 mg of NT was added to 100 mg of the molten lipid ($80 \pm 2^{\circ}C$; under continuous magnetic stirring at 2000 rpm for 10 mins), and the NT-lipid mix was cooled. All the NT-lipid mixes were then microscopically observed for the precipitation of NT, and the lipids which did not show any precipitation were selected. Precirol® ATO 5 and castor oil were found to be the most suitable lipids, in which NT showed no precipitation.

Experimental Design

Box-Behnken design was employed in the experimental design where the amount of castor oil, Precirol® ATO 5, Span® 80, and high-pressure homogenization (HPH) time were varied at 3 levels as hypothesized by the design. In the given study, the abovementioned 4 factors were taken as the independent factors (coded as A, B, C, and D, respectively, at 3 different levels), whereas, formulation characters such as particle size, polydispersity index (PDI), % drug entrapment, and % drug loading (DL) were considered as the response variables (dependent variables). Tables 1 and 2 provide the details on the Box-Behnken experimental design employed in this study.

The general form of the model generated from the design is given below,

$$Y = \beta_0 + \beta_1 A + \beta_2 B + \beta_3 C + \beta_4 D + \beta_5 AB + \beta_6 AC + \beta_7 AD + \beta_8 BC + \beta_9 BD + \beta_{10} CD + \varepsilon \quad (1)$$

where β_0, the intercept, is the arithmetic average of all quantitative outcomes of 25 experimental runs, β_1-β_{10} are the coefficients computed from the observed experimental values of Y, and A, B, C, and D are the coded levels of the independent factors. The A, B, C, and D terms indicate the average result of changing one factor at a time from its low to high value. The interaction terms (AB, AC, AD, BC, BD, and CD) suggest the response changes when 2 factors are changed simultaneously. The equation aids in understanding the effect of the independent factor/s on the response variables after considering the intensity of coefficient and the mathematical sign it carries, that is, positive or negative. A positive sign indicates additive effect. Statistical validity was established based on ANOVA provided in the Design-Expert® software, with level of significance considered at $p < 0.05$.

Formulation Optimization

Response surface methodology (RSM) computations including 3-dimensional (3-D) RSM, interaction, and contour plots for the

Table 3
Results From Solid and Liquid Lipid Screening (Drug and Lipids Added in 1:1 Ratio at 80 ± 2°C; Under Continuous Magnetic Stirring at 2000 rpm for 10 min)

Solid/Liquid	Lipid	Solubility
Solid lipids	Glyceryl monostearate	(−)
	Precirol® ATO 5	(+)
	Compritol® 888 ATO	(−)
Liquid lipid	Castor oil	(+)
	Olive oil	(−)
	Sesame oil	(−)
	Soybean oil	(−)
	Oleic acid	(−)
	Labrafac® lipophile WL 1349	(−)
	Maisine® CC	(−)
	Miglyol® 829	(−)
	Captex® 355 EP	(−)

(+), NT is soluble in the lipid melt and does not precipitate on cooling; (−), NT is either soluble in the lipid but precipitates on cooling or is insoluble in the lipid.

formulation optimization were performed using Design-Expert® software (8.0.7.1) to obtain optimum values of the response variables based on the criteria of desirability (Table 1). The optimum variables were used to prepare the suggested optimum formulation; the predicted and experimental values for the suggested formulation were then compared to validate the chosen experimental design and the models.

Preparation of NT-PEG-NLCs

The NT-PEG-NLCs were prepared by the hot homogenization method. An aqueous (AH) phase was prepared using surfactants such as poloxamer 188 (0.25% w/v), Tween® 80 (0.75% w/v), and glycerin (2.25% w/v) in deionized water, and this was heated and added to the molten lipid phase under stirring form a premix (2000 rpm, 5 min). The lipid phase consisted of NT (0.3%), Precirol® ATO 5, castor oil, Span® 80, and mPEG-2K-DSPE sodium salt. The premix was then emulsified at 16,000 rpm for 5 min using T 25 digital Ultra-Turrax to form a hot preemulsion. The preemulsion obtained was subjected to HPH (15,000 psi) using thermostated EmulsiFlex C5 (Avestin®) resulting in the formation of hot emulsion dispersion. The temperature during the entire process was maintained at 80 ± 2°C. The hot emulsion obtained was cooled to room temperature to form the NT-PEG-NLCs.

Particle Size and PDI

The hydrodynamic radius and PDI of the NT-PEG-NLC formulations were determined by photon correlation spectroscopy using a Zetasizer Nano ZS Zen3600 (Malvern Instruments, Inc.) at 25°C and with 173° backscatter detection in disposable folded capillary clear cells. The measurements were obtained using a helium-neon laser, and the particle size analyses data were evaluated based on the volume distribution. Briefly, 10 μL of the sample was diluted to 1000 μL using deionized water, and the particle size and PDI were measured.

Morphological Characteristics Using Scanning Tandem Electron Microscopy

A 20-μL drop of sample was placed on a sheet of clean parafilm. A freshly glow-discharged 200-mesh copper grid coated with a thin carbon film was floated film side down on the drop of sample. After 30 s, the grid was removed from the drop, and excess sample was removed by touching a piece of filter paper to the edge of the grid. Before complete drying, the grids were placed sample side down on a drop of ultrapure water and immediately removed; excess water was removed and the grid, sample side down, was placed on a drop of 1% uranyl acetate. After 1 min, the grid was removed from the drop, and excess stain was removed. The grid with sample was dried completely before examination in a Zeiss Auriga® operating in scanning tandem electron microscopy (STEM) mode at 30 kV (studies performed at the University of Tennessee, Knoxville, TN).

Powder X-Ray Diffraction Analysis

A qualitative powder X-ray diffraction (PXRD) was done (studies performed at the Campbell University, Buies Creek, NC) to examine the physical state of NT in the formulated NT-PEG-NLC. The X-ray powder diffraction patterns of the samples were recorded with the Rigaku Ultima IV X-ray diffractometer using Ni-filtered, CuKα radiation generated at 40 kV and a current intensity of 44 mA. The diffraction angle range of the instrument was operated over a range of 2θ angles from 5° to 50°.

Physiochemical Stability

Physical and chemical stability of the optimized formulation was evaluated by analyzing the changes in particle size, PDI, assay, and % entrapment efficiency upon storage at 4°C and 25°C for a period of 1 month.

NT Content (Assay), Entrapment, and Load

Assay. An accurately measured amount of NT-PEG-NLC (10 μL) was extracted in methanol (990 μL) because NT is soluble in methanol. The methanol-formulation mixture was then centrifuged at high speed (13,000 rpm, 15 min), and the resulting supernatant was analyzed for NT content using HPLC method. The NT drug content (assay) was used in the determination of the percentage of NT entrapped in the nanoparticles.

Entrapment. A measured amount of NT-PEG-NLC formulation (500 μL) was taken and placed in the centrifugal filter (100 kDa), and the sample was centrifuged at a high speed (13,000 rpm, 15 min), after which the filtrate was collected and analyzed for free NT content. Percentage NT entrapped was calculated using the formula,

$$\%\ \text{entrapment} = \frac{(\text{Amount of drug determined in assay} - \text{Amount of untrapped drug})*100}{\text{Amount of drug weighed}} \quad (2)$$

Loading. The amount of NT load in the NT-PEG-NLC formulation was determined by the following formula,

$$\%\ \text{drug load} = \frac{\text{Amount of drug entrapped}}{\text{Total lipid content}} \times 100 \quad (3)$$

Analysis of In Vitro *Samples.* NT was quantified using a validated HPLC method reported in literature.[18] The HPLC system consisted of a Waters 717 plus Autosampler coupled with a Waters 2487 Dual λ Absorbance UV detector, a Waters 600 controller pump, and an Agilent 3395 Integrator. The mobile phase consisted of a mixture of phosphate buffer (0.2 M, pH 5.5) and acetonitrile (70:30) with flow rate of 1 mL/min. A C18 Phenomenex Luna® (5 μ, 250 × 4.6 mm)

Table 4
Summary of Regression Analyses Performed by Design-Expert® Software for Evaluating the Effects of Independent Factors on the Response Variables

Response Variable	Model	Model F Value	Degree of Freedom	R^2 Values	
				R^2	Adjusted R^2
Particle size	2FI	5.27	6	0.6372	0.5163
PDI	2FI	NA	NA	NA	NA
% entrapment	2FI	6.75	4	0.5746	0.4895
% DL	2FI	15.36	4	0.7544	0.7053

column was used. The temperature for the analyses was 25°C, the injection volume was 20 μL, and the UV detection wavelength was set to 304 nm at AUFS 1.00.

In Vitro *Transcorneal Permeation*

Transmembrane permeability of NT from NT-PEG-NLC formulation was evaluated across isolated rabbit cornea (Pel-Freez Biologicals®) using vertical diffusion cells (PermeGear®, Inc.). To compare and evaluate the effect of PEGylation, NT-NLCs without the PEG component were prepared, and their transmembrane corneal permeability was assessed (1.5% w/v of PEG was replaced by 1.5% w/v of Precirol® ATO 5; NT load was kept constant at 0.3% w/v).

The cornea was clamped in between the 2 half cells with the epithelial surface facing upward toward the half cell with less volume (i.e., the donor cell containing the formulations). Natacyn® (5% w/v), NT-PEG-NLCs (0.3% w/v), and NT-NLCs (0.3% w/v) were used as donor formulations; 5% Natacyn® was diluted using Dulbecco's phosphate-buffered saline (DPBS) to 0.3% w/v to dose normalize all 3 formulations. Five milliliters of 2.5% solution of randomly methylated β-cyclodextrin in DPBS was used in the receiver compartment. The contents of the receiver chamber were stirred continuously with a magnetic stirrer. Aliquots (200 μL) were withdrawn from the receiver chamber at predetermined time points and replaced with an equal volume of 2.5% w/v randomly methylated-β-cyclodextrin in DPBS. The study duration was 3 h. The concentration of NT in the receiver chamber solution was determined using the HPLC analyses method for *in vitro* samples described previously.

In Vivo *Ocular Biodistribution Studies*

In vivo BA of NT was determined in male New Zealand white albino rabbits, weighing between 2 and 2.5 kg, procured from Charles River Laboratories. All the animal studies conformed to the tenets of the Association for Research in Vision and Ophthalmology statement on the use of animals in ophthalmic vision and research, and the University of Mississippi Institutional Animal Care and Use Committee approved protocols. The NT formulations, such as the NT-PEG-NLC, NT-NLC, and Natacyn® (0.3% and 5%), were evaluated in conscious rabbits, *in vivo* ($n = 4$). All the aforementioned NT topical formulations (100 μL) were given as 2 doses (50 μL) every 2 h for a 6-h time period (t = 0, 2, and 4 h). Two hours after the third instillation at t = 6 h, the rabbits were anesthetized using a combination of ketamine (35 mg/kg) and xylazine (3.5 mg/kg) that was injected intramuscularly. The rabbits were euthanized with an overdose of pentobarbital injected through a marginal ear vein. The eyes of the rabbits were then enucleated and washed thoroughly with isotonic phosphate buffer saline, and the intraocular tissues such as cornea, iris-ciliary body (ICB), AH, and vitreous (VH) humors were separated.

A protein precipitation technique was employed to determine the amount of NT in the ocular tissue homogenates. Briefly, the solid tissues such as cornea and ICB (cut into small pieces) and the liquid tissues such as AH and VH (taken as they were) were taken, and ice-cold methanol was added (0.6 mL) to precipitate proteins from each individual tissue. The supernatant was then collected via centrifugation for 0.5 h at 13,000 rpm before the analyses.

Quantification of NT was performed using standard calibration curves constructed from various ocular tissues, such as the cornea (0.6-131.1 ng/mL), the ICB (0.6-65.5 ng/mL), the AH (2-400 ng/mL), and the VH (2-400 ng/mL), using the LC-MS/MS method. All the standard curves had a coefficient of determination $r^2 \geq 0.96$. The extraction recovery (extraction efficiency) of NT was higher than 95% for cornea, ICB, and AH, whereas it was about 82% for VH. The process efficiency was higher than 90% for all the tissues. Interference was not observed from coeluted protein residues with respect to NT peaks in any of the tissues. The limit of detection for various ocular tissues was determined and corresponded to 0.13 ng/mL for all the 4 tissues.

Quantification of NT in the Biosamples

For quantification of NT in the *in vivo* samples, a Waters Xevo TQ-S triple quadrupole tandem mass spectrometer with an electrospray ionization (ESI) source, equipped with the ACQUITY UPLC® I-Class System, was used (Waters Corporation, Milford, MA). Data

Table 5
ANOVA for Response Surface Reduced 2FI Model

Response Variables	Independent Factors that Affect the Response Variable Significantly	*p* Value	Final Equation in Terms of Coded Factors Fitted in 2FI Model
Particle size	A	0.0058	Particle size = 231.07 + 28.48*A + 14.55*B − 3.43*C − 20.928*D − 38.38*AD − 44.45*BC (Eq. 1)
	D	0.0338	
	AD	0.0256	
	BC	0.0114	
% entrapment	A	0.0046	% entrapment = 91.29 − 16.07*A + 12.03*B + 11.04*D − 21.86*BD (Eq. 2)
	B	0.0268	
	D	0.0401	
	BD	0.0209	
% DL	A	<0.0001	% DL = 5.89 − 2.92*A + 0.08*B + 0.73*D − 1.49*BD (Eq. 3)
	BD	0.0435	

A, Precirol® ATO 5; B, castor oil; C, Span® 80; D: HPH time; AD, interaction between Precirol® ATO 5 and HPH time; BD, interaction between castor oil and HPH time; BC, interaction between castor oil and Span® 80.

acquisition was performed with Waters Xevo TQ-S quantitative analysis TargetLynx software, and data processing was executed with MassLynx mass spectrometry software. Separation operations were accomplished using a C18 column (Acquity UPLC® BEH C18 100 mm × 2.1 m, 1.7-µm particle size). The mobile phase consisted of water (A) and acetonitrile (B), both containing 0.1% formic acid at a flow rate of 1.0 mL/min, with a gradient elution as follows: 0 min, 98% A/2% B held for 0.2 min, and 100% B in next 2.3 min. Each run was followed by a 1-min wash with 100% B and an equilibration period of 2 min with 98% A/2% B. The column and sample temperature were maintained at 50°C and 10°C, respectively. The effluent from the LC column was directed into the ESI probe. Mass spectrometer conditions were optimized to obtain maximal sensitivity. The following conditions were used for the ESI source: source temperature 150°C, desolvation temperature 600°C, capillary voltage 3.0 kV, cone voltage 40 V, nebulizer pressure 7 bar, and nebulizer gas 1100 $L \cdot h^{-1}$ N_2. Argon was used as the collision gas. The collision energies were optimized and ranged from 10 to 15 eV for individual analytes. Instrument control and data processing were performed by using MassLynx software (version 4.1; Waters, Milford, MA). Mass spectra were acquired in positive mode and multiple reactions–monitoring mode. The multiple reactions–monitoring mode was applied to monitor the transitions of quantifier ion to qualifier ions (the precursor to fragment ions transitions) of *m/z* 666.2 → *m/z* 467.2, 485.2, 503.2 for NT and of *m/z* 924.4 → *m/z* 107.5, 743.2, 761.4 for amphotericin B. Amphotericin B was used as the internal standard. Confirmation of compounds was achieved through 3 fragment ions.

Statistical Analyses

Data are represented as the mean ± standard deviation, for a minimum of 3 independent experimental runs. Statistical comparisons of the means were performed using one-way ANOVA or Student's *t*-test. The differences were considered to be significant when the *p* value was <0.05.

Results

Lipid Screening Study

The results observed from solid and liquid lipid screening are presented in Table 3. On the bases of the following results, castor oil and Precirol® ATO 5 were chosen as the lipids for the preparation of NT-PEG-NLCs and NT-NLCs.

Formulation Development and Optimization Using Box-Behnken Method

The 25 NT-PEG-NLC formulations that were prepared according the Box-Behnken design were analyzed for particle size, PDI, % NT entrapment, and % DL. The Design-Expert® software was used to study the effect of content of lipids (castor oil and Precirol® ATO 5), Span® 80, and HPH time (independent factors) on the above-mentioned responses (particle size, PDI, % entrapment, and % DL). The extent of the effect of the independent factors on the response variables was determined using the regression analyses and plots that provided RSM analyses. Tables 4 and 5 elucidate the results of the regression analyses, and Figures 1-4 display the 3D RSM, interaction, and contour plots, respectively.

The optimum formulation was generated by the numerical optimization technique following desirability approach using the Design-Expert® software. The output for the most desirable formulation for NT-PEG-NLCs generated by the software is given in

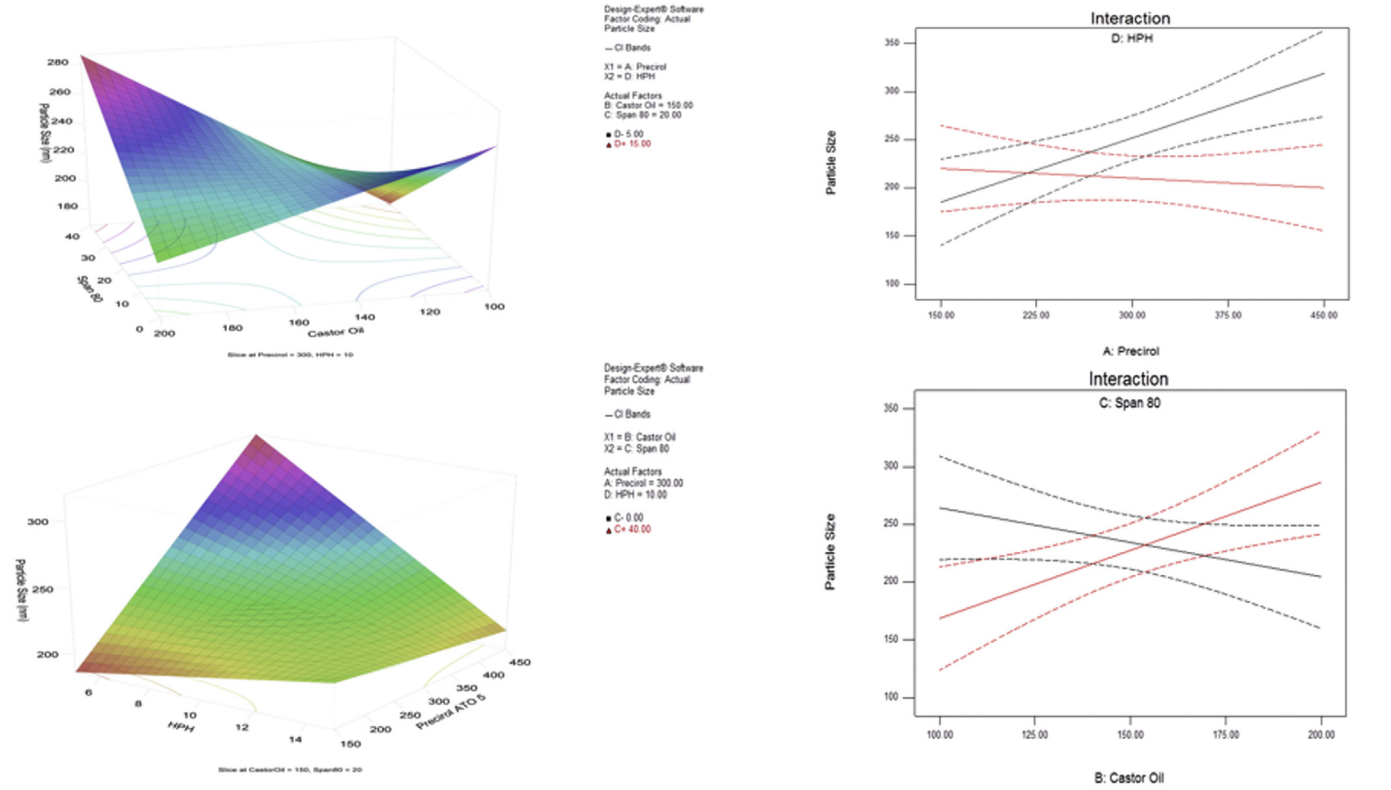

Figure 1. RSM, interaction, and contour plots showing the effect of Precirol® ATO 5, castor oil, Span® 80, and HPH time on particle size and plot between the observed and predicted values of particle size.

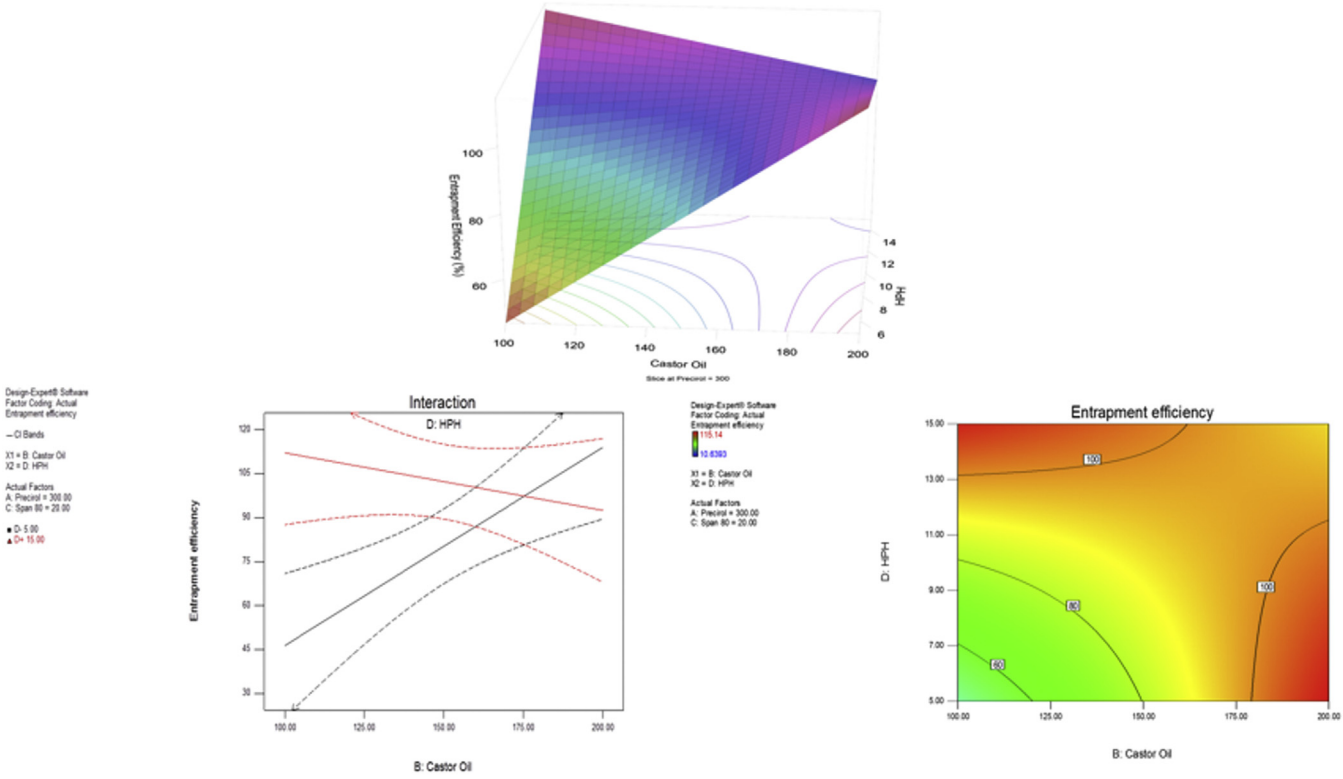

Figure 2. RSM, interaction, and contour plots showing the effect of castor oil and HPH time on % entrapment and plot between the observed and predicted values of % entrapment.

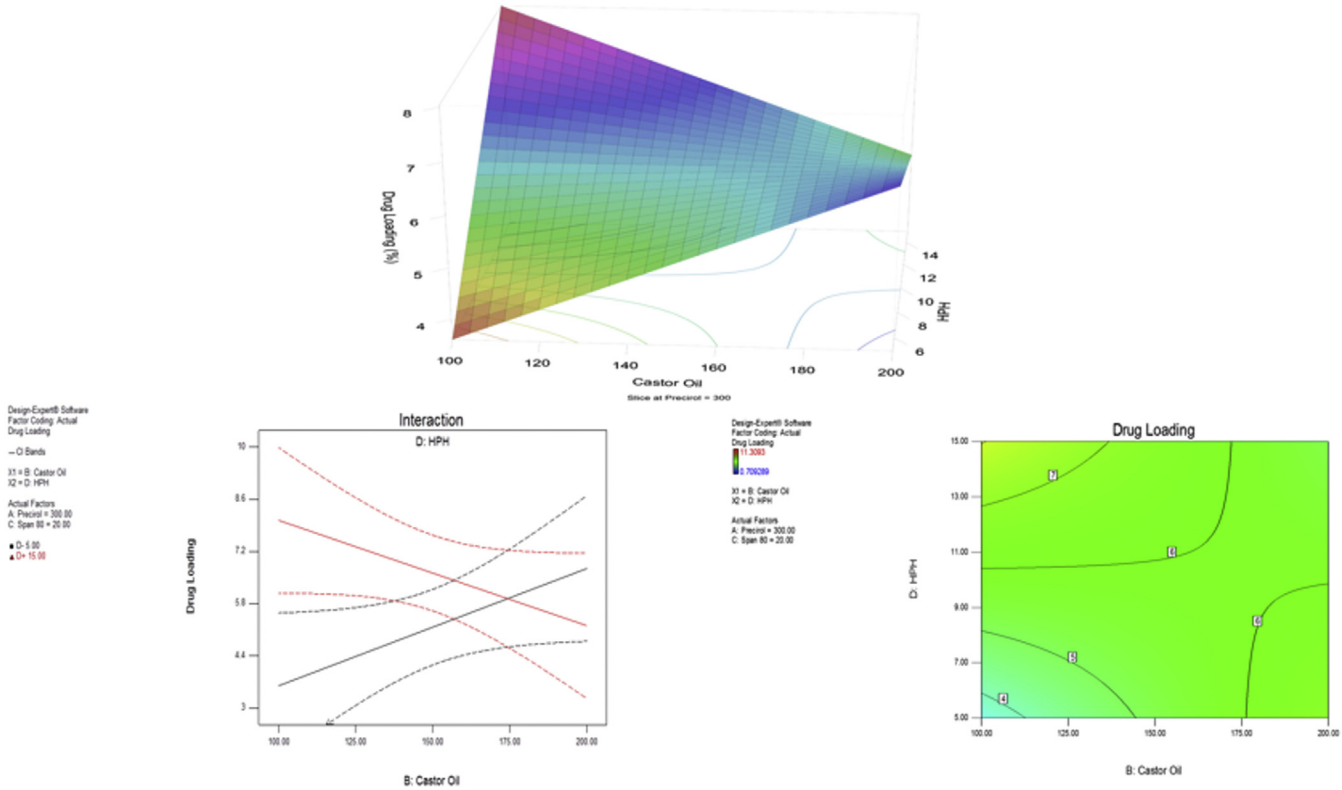

Figure 3. RSM, interaction, and contour plots showing the effect of castor oil and HPH time on % DL and plot between the observed and predicted values of % DL.

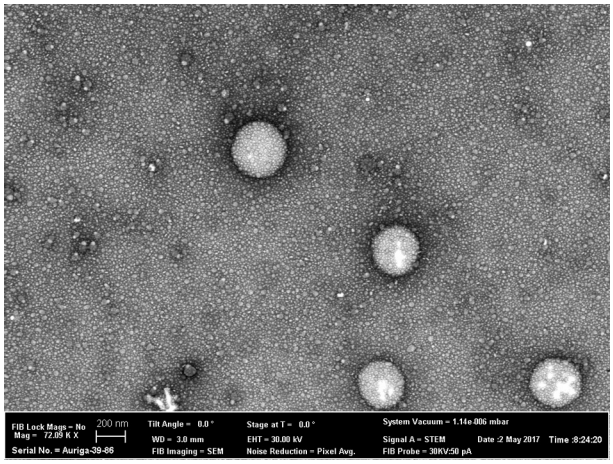

Figure 4. STEM image for the optimized NT-PEG-NLC formulation.

Table 6. Table 6 also enlists the predicted values for the responses and the values that were observed experimentally for the most suitable formulation that had a desirability of 0.9835.

Morphological Characterization Using STEM

Figure 4 depicts the morphology of the NT-PEG-NLC which was found to be spherical upon STEM imaging with particle size in the range of 200-250 nm.

PXRD Analysis

Figure 5 represents the PXRD stacked plots. The PXRD plots revealed the absence of characteristic NT peaks at 2θ values of 11.95, 15.25, 16.80, and 17.81 in the NT-PEG-NLC (highlighted within black circles).

Physiochemical Stability

The optimized formulation did not show any particle aggregation upon visual inspection, until 4 weeks at both the temperature conditions. From Figure 6, it can be concluded that the NT-PEG-NLCs did not show any statistically significant changes in particle size, PDI, and %NT entrapment during its storage for 1 month at 4°C and 25°C ($p > 0.05$).

In Vitro *Transcorneal Permeation*

The transcorneal permeability of NT from the NT-PEG-NLCs, NT-NLCs, and Natacyn® were observed to be $(0.114 \pm 0.04) \times 10^{-5}$, $(0.06 \pm 0.02) \times 10^{-5}$, and $(0.014 \pm 0.01) \times 10^{-5}$ cm/s, respectively (Fig. 7). The transcorneal flux of NT was approximately 2 and 7 times higher from NT-PEG-NLCs in comparison to NT-NLCs and Natacyn®, respectively (Fig. 7). Accordingly, the trend for rate of permeation was observed to be NT-PEG-NLCs > NT-NLCs > Natacyn® (Fig. 7).

In Vivo *Ocular Biodistribution Studies*

Based on the *in vitro* transcorneal permeation, the NT formulations were investigated for their ocular biodistribution of NT upon topical application in conscious rabbits having intact corneal epithelium. All the NT formulations could deliver the drug to cornea, ICB, AH, and VH which are the most common sites for OFI. The ocular tissue NT concentrations obtained from the above formulations are shown in Figure 8.

In cornea, the NT concentration from Natacyn® (5%) was significantly higher than that from NT-PEG-NLC ($p < 0.05$). However, when Natacyn® was diluted and administered at 0.3% (dose normalized with NT-PEG-NLC), a significantly higher concentration was obtained for NT from NT-PEG-NLC in comparison to diluted Natacyn® (0.3%) ($p < 0.05$). In addition, a statistically significant difference was found between the NT concentrations from NT-PEG-NLC and NT-NLC in cornea ($p < 0.05$).

The concentration of NT from NT-PEG-NLC and Natacyn® (5%) in ICB was found to be statistically nonsignificant ($p > 0.05$). However, a statistically significant difference was found in ICB for the NT concentrations from NT-PEG-NLC and diluted Natacyn® (0.3%) at their dose-normalized concentrations. Similar to cornea, in ICB too, a statistically significant difference was found between the NT concentrations obtained from NT-PEG-NLC and NT-NLC.

The concentration of NT from NT-PEG-NLC, NT-NLC, and Natacyn® (0.3% and 5%) did not show a statistically significant difference in AH. However, in VH, a statistically significant difference was observed in NT concentrations obtained from NT-PEG-NLC and Natacyn® (5%), with higher NT concentration from NT-PEG-NLCs.

Discussion

Currently, NT is the only marketed antifungal drug that is indicated in the management of OFI-like fungal keratitis and fungal endophthalmitis.[19] One of the major challenges that is associated with the commercial NT formulation is the low BA (~2%) that necessitates the frequent ocular application (about 6-8 times a day) of the NT commercial formulation.[8] Hence, to potentially improve its BA and enhance its permeation into the ocular tissues, a surface-modified (using mPEG-2K-DSPE) NLC system for NT was developed. The primary objective of this investigative study was to develop, optimize, and characterize the optimized PEGylated lipid-based nanoparticulate dosage system for the ocular delivery of NT and to investigate its corneal permeation, *in vitro* and *in vivo*.

Nano-lipid drug carriers are colloidal nanoparticulate dispersions that can be administered topically in the form of eye drops. A major advantage of the nanoparticulate systems over the

Table 6
Composition of the Most Desirable Formulation Obtained by Design-Expert® Software With Predicted and Experimental Values

Formulation Composition of the Most Desirable Formulation	Predicted Values	Experimental Values
NT (0.3% w/v)	Particle size: 225.01	Particle size: 241.96
Castor oil (1% w/v)	PDI: 0.410	PDI: 0.406
Precirol® ATO 5 (1.5% w/v)	% entrapment: 100.00	% entrapment: 95.35
mPEG-2K-DSPE sodium salt (1.5% w/v)	% DL: 7.96	% DL: 6.45
Span® 80 (0.11% w/v)	Desirability: 0.9835	NT content: 97.85%
Poloxamer 188 (0.25% w/v)		
Glycerin (2.25% w/v)		
Tween® 80 (0.75% w/v)		

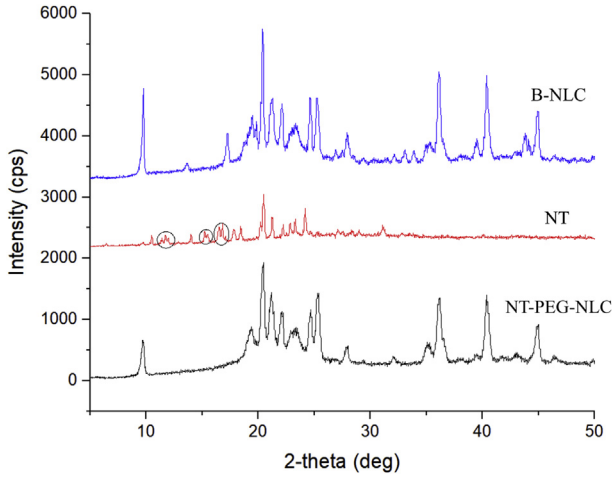

Figure 5. PXRD plots for B-NLC (PEG-NLC without NT), NT, and NT-PEG-NLC.

conventional drug delivery systems is that their uptake is facilitated by epithelial cells, which allows for greater penetration into and from the corneal surface.[20-23] Moreover, their small size, biocompatibility, and chemically inert nature improves their interactions and prolongs the preocular residence time of drugs, thus enhancing drug BA.[24-27] Surface modification of NLCs by coating with hydrophilic agents such as PEGs and PEG derivatives, in addition to improving the pharmaceutical stability of the system, can further enhance ocular penetration, mainly increasing the cellular uptake and internalization.[28-31]

Castor oil and Precirol® ATO 5 were chosen as the liquid and solid lipids because NT had the highest solubility in them without causing any precipitation upon cooling the NT-lipid melt. Span® 80, a surfactant, was chosen to achieve the highest loading for NT, reduce the particle size, and obtain a narrow PDI distribution. The content of mPEG-2K-DSPE sodium salt was kept constant at 1.5% w/v in all the experimental trails because, in our previous studies, 1.5% w/v content of mPEG-2K-DSPE sodium salt was found to be the most optimum load that could stabilize the NLC system and enhance the corneal drug permeation upon topical instillation.[17]

In the formulation development and optimization process, the most suitable formulation was selected using the Design-Experiment® software that used the Box-Behnken design. The Box-Behnken design was chosen over the traditional factorial design methods because the Box-Behnken design sharply reduces the number of experimental runs without decreasing the accuracy of the optimization process. Regression analyses, 3D RSM, interaction, and contour plots provided by the software aided in understanding the effect and interaction of the independent factors on the response variables. These effects and/or interactions served as bases in selecting the most optimum formulation as a predicted outcome from the software.

In predicting the most optimum formulation from the 25 experimental trials using Design-Expert® software, formulations were analyzed for particle size, PDI, % entrapment, and % DL. The optimized formulation had the constraints that it should have the highest entrapment and % DL, particle size at the lower spectrum of 10-1000 nm (<300 nm), and a narrow PDI. A higher entrapment and DL is sought for delivering a higher amount of drug at the ocular site, and particle size at the lower spectrum of 10-1000 nm with a narrow PDI is required for the penetration of the drug-loaded nanoparticles from the ocular surface.[24]

Regression analyses, 3D RSM, interaction, and contour plots provided by the Design-Expert® software aided in understanding the effect of the excipients and processing parameters on the physicochemical attributes of the NT-PEG-NLC formulation. The independent factors (amount of excipients and processing time)

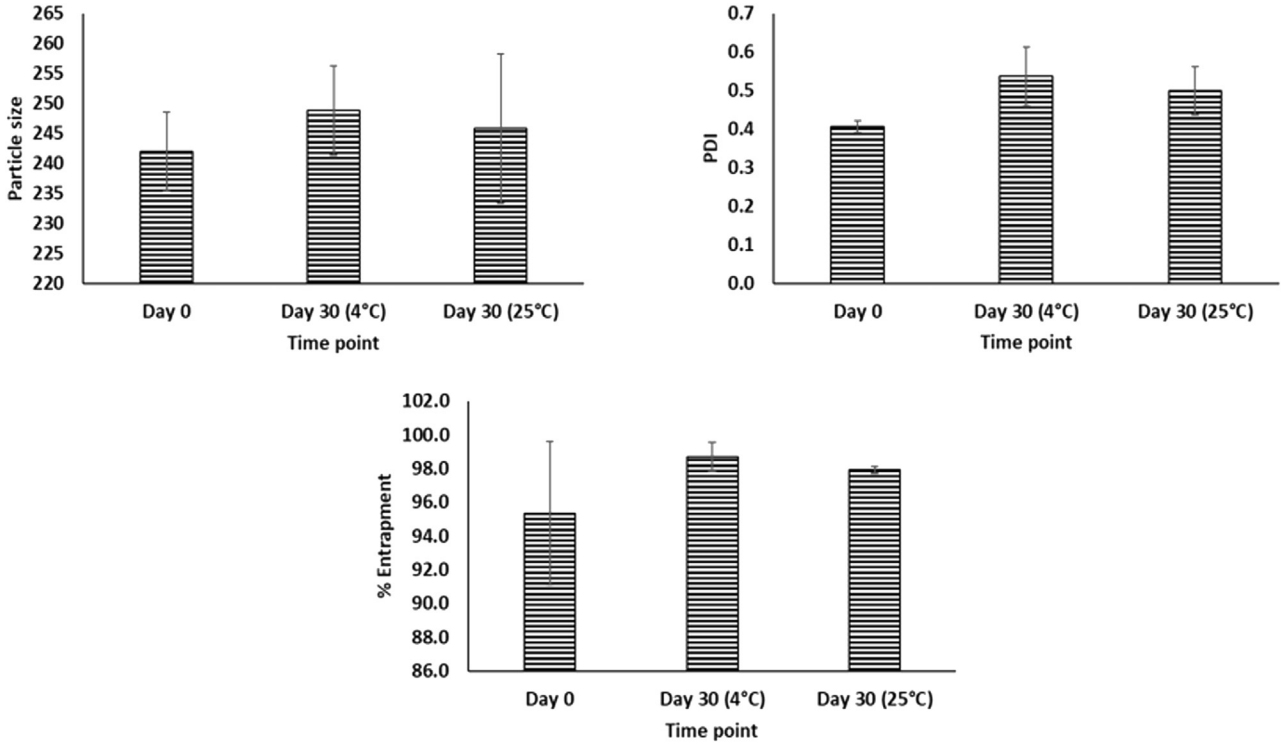

Figure 6. Plots showing changes in particle size, PDI, and % NT entrapment for the NT-PEG-NLC formulation for 1 month at 4°C and 25°C. The changes are statistically nonsignificant at $p > 0.05$.

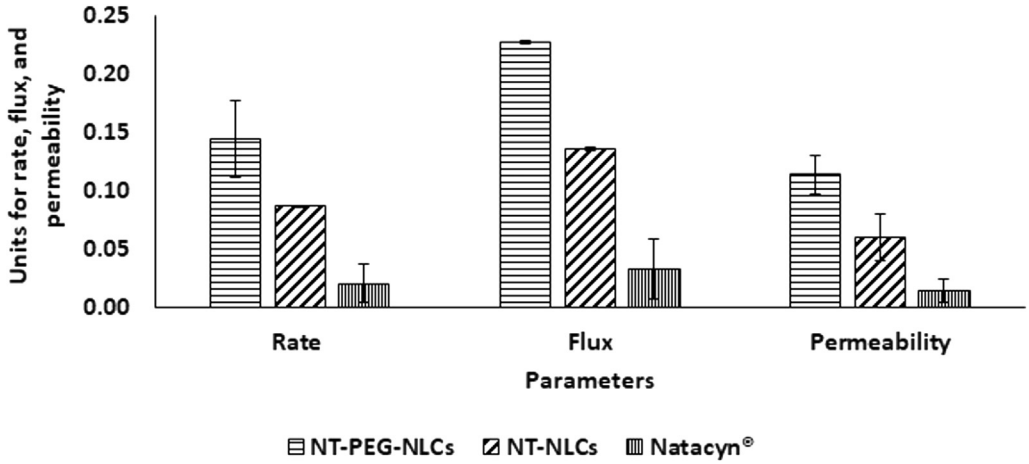

Figure 7. Plot of rate (μg/min), flux (μg/min/cm^2), and permeability ($\times 10^{-5}$ cm/s) for NT permeation across the cornea from NT-PEG-NLCs, NT-NLCs, and Natacyn® over 3 h, ($n = 3$). The data for rate, flux, and permeability show a statistically significant difference at $p < 0.05$ for NT-PEG-NLCs, NT-NLCs, and Natacyn®.

were fit into a 2FI (2 factor interaction) model, and the 2FI models were found to be significant for particle size, % entrapment, and % DL; high F values for 2FI models indicate a strong effect of amount of excipients and processing time on the physicochemical attributes (particle size, % entrapment, % DL) of the final NT-PEG-NLCs (Table 4). Accordingly, the content of lipids (Precirol® ATO 5 and castor oil), surfactant (Span® 80), and processing parameter (HPH time), individually and/or in combination, were found to affect the particle size, % NT entrapment, and % DL of NT-PEG-NLC formulation. An in-depth discussion on the effect of excipients and processing parameters on the NT-PEG-NLC formulation characteristics has been individually elaborated in the following sections.

The particle size of the NT-PEG-NLC was found to be significantly affected by the amount of Precirol® ATO 5, HPH time, and interactions between (Precirol® ATO 5 and HPH time) and (castor oil and Span® 80) ($p < 0.05$). Particle size was found to increase with an increase in the amount of lipid excipients (Precirol® ATO and castor oil) and decrease with an increase in the amount of surfactant (Span® 80) and processing time (HPH time). From Equation 1 of Table 5, it is observed that an increase in the amount of Precirol® ATO 5 and a shorter HPH time will lead to an increase in the particle size. It has been evidenced that an increase in the amount of solid lipid in the NLC system increases the particle size because of an increase in the lipid density.[32,33] Also, a shorter duration of homogenization versus a longer duration leads to the application of lower shear resulting in NLCs having a higher particle size.[32,33] From the plots in Figure 1, the combined interaction of Precirol® ATO 5 and HPH time with castor oil and Span® 80 could be explained. The effect of combined interaction of Precirol® ATO 5 and HPH time affected the particle size in a pattern like the effect

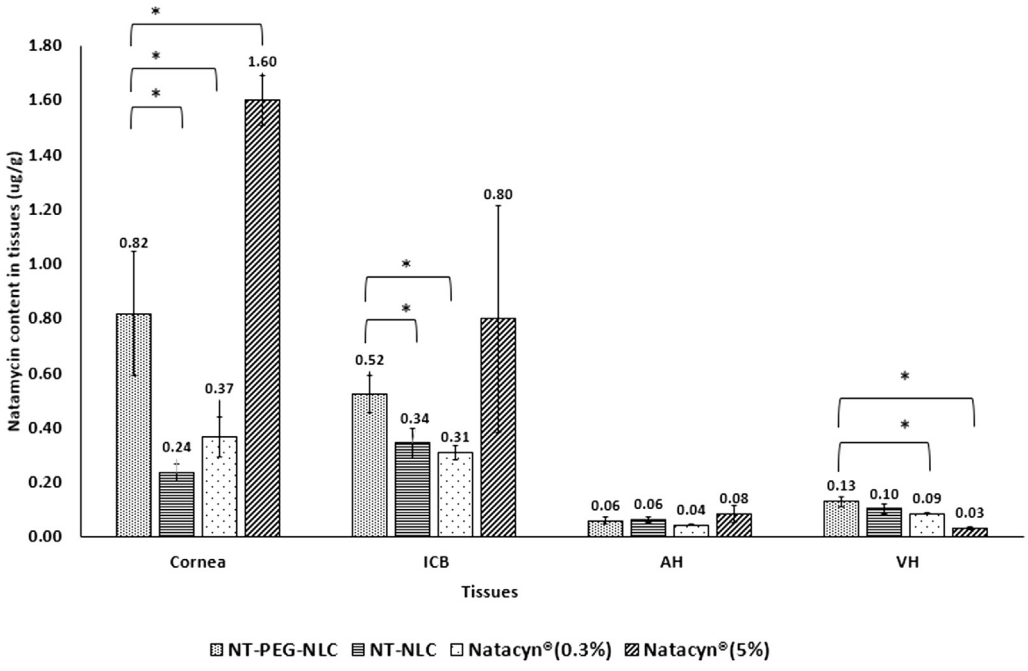

Figure 8. NT concentrations (μg/g) in cornea, ICB, AH, and VH from NT-PEG-NLC, NT-NLC, and Natacyn® (0.3% and 5%) obtained after 3 doses; administered every 2 h (t = 0, 2, and 4 h) for a 6-h study; (*) denotes statistically significant difference at $p < 0.05$ ($n = 4$, data represented as mean ± standard error).

observed for the 2 factors individually. The effect of the combined interaction of Span® 80 and castor oil was found to affect the particle size, with the lowest amounts of castor oil and the highest amount of Span® 80 giving the lowest particle size. A lower liquid lipid results in lower density of the lipid in the system, and a higher amount of surfactant promotes formation and stabilization of the NLC by decreasing the interfacial tension between the lipid and the external phase.[32,34]

PDI was one of the response factors in deciding the most optimum formulation. However, a mathematical model could not be generated for it. The variation in PDI was extremely narrow and did not vary significantly. The absence of the mathematical model for PDI indicated that the hot homogenization method was robust to the changes in independent factors, and hence, any changes in the independent factors did not significantly affect the responses for PDI.

It was found that % entrapment was significantly (p <0.05) affected by the amount of Precirol® ATO 5, castor oil, HPH time, and interactions between castor oil and HPH time (Table 5, Eq. 2). An increase in the amount of liquid lipid (castor oil), increase in the processing time (HPH time), and a decrease in the amount of solid lipid (Precirol® ATO 5) was found to improve the entrapment of NT in the NT-PEG-NLCs. From Equation 2 of Table 5 and Figure 2, it is observed that the amount of castor oil, duration of homogenization, and their combined interaction linearly affects the entrapment of NT. An increase in NT entrapment by increasing the amount of castor oil and duration of homogenization, either individually or in combination, causes an increase in the surface area of castor oil in the presence of a surfactant (Span® 80) during the homogenization process which may lead to a higher partition of NT (a lipophilic drug) into the castor oil phase, thereby improving the drug entrapment.[35] In NLCs, because the solid lipid forms the outer matrix, an increase in the amount of Precirol® ATO 5 (solid lipid) could lead to reduced entrapment of NT within the NLC core (containing the castor oil) and higher presence of NT on the surface of NLCs.[36]

The amount of Precirol® ATO 5 and the combination of interaction between castor oil and HPH time were found to have an effect on the DL. An increase in % DL was observed with a decrease in the amount of Precirol® ATO 5 and an increase in the HPH processing time. An increase in the amount of solid lipids without increasing the liquid lipid amounts are reported to reduce the DL owing to the denser matrix provided by the solid lipids; hence, increasing the amount of Precirol® ATO 5 (solid lipid) without increasing the castor oil amount leads to a reduction of NT load in the NLC system (Table 5, Eq. 3).[36,37] Similarly, the HPH time and the interaction factor involving it affect the NT load proportionally. A longer duration of homogenization leads to an increase in the % DL as observed from Equation 3 of Table 5 and Figure 3 plots. This could possibly occur on account of the increased surface area available during the prolonged homogenization process that could lead to a higher drug load.[32]

Upon understanding the effects of excipients and processing parameters on the formulation attributes such as particle size, PDI, % entrapment, and % DL, an optimized formulation was suggested by the Design-Expert® software. Using desirability approach, the optimum formulation was selected and formulated, and a close agreement between the predicted values and experimental values for particle size, PDI, % entrapment, and % DL was observed (Table 6).

The particle size of NT-PEG-NLCs, using STEM, was found to be approximately in the range of 200-250 nm, which was in agreement with the particle size dimensions obtained from dynamic light scattering experiments (Fig. 4). In determining the physical state of NT in NT-PEG-NLC using a qualitative PXRD method, absence of characteristic NT peaks in NT-PEG-NLC (Fig. 5) indicates a potential amorphous transition of NT and/or its entrapment within the lipid matrices. Physical stability of the formulation is an important characterization parameter that could be evaluated by the changes in particle size, PDI, and % drug entrapment.[34] The statistically nonsignificant changes in the abovementioned parameters for the optimized NT-PEG-NLCs suggested that the nanoparticulate system was stable for 1 month at 4°C and 25°C.

The topical medications instilled into the eye majorly undergo absorption via the corneal route.[38] Compared to Natacyn®, both NT-PEG-NLCs and NT-NLCs demonstrated significantly higher permeability across the cornea, *in vitro*. This could be attributed to the endocytosis-mediated internalization of the NT-NLCs and NT-PEG-NLCs, leading to their higher permeation across the cornea and lower retention within the cornea in comparison to Natacyn®.[38-40] In case of NT-NLCs and NT-PEG-NLCs, the latter showed a higher transcorneal permeation. The higher *in vitro* transcorneal permeability of NT-PEG-NLCs is in agreement with the reported literature (PEGylated nanocarriers penetrating better across the corneal epithelium and mucosa than their non-PEGylated counterparts) and could be ascribed to the strong hydrophilicity provided by the PEG coating, which aids in the quicker diffusion of NT-PEG-NLCs in comparison to the NT-NLCs (devoid of PEG coating).[30,41,42] An earlier report from our laboratory has demonstrated the effect of PEGylation and also evaluated the effect of PEG chain length and PEG density on the transcorneal permeability.[43] Thus, in this study, in terms of *in vitro* transcorneal permeability, the NT-PEG-NLCs > NT-NLCs > Natacyn®.

A couple of studies have evaluated NT-loaded nanoparticle formulations. The development and characterization (*in vitro* and *in vivo*) of NT-loaded poly-D-glucosamine functionalized polycaprolactone nanoparticles and NT-loaded lecithin-chitosan mucoadhesive nanoparticles at 1% and 5% w/v of NT loading, for ophthalmic keratitis, have been reported by Chandasana et al. and Bhatta et al., respectively. In both these studies, it was found that the NT nanoparticles (1% and 5% w/v) demonstrated improved tear pharmacokinetic profiles such as higher concentration, greater area under curve, higher residence times, and lower clearance in the lacrimal fluid and at the precorneal sites in comparison to the marketed NT suspension (5% w/v).[44,45] However, the authors did not investigate/report NT concentrations in the surface or inner ocular tissues. In another evaluation by Paradkar et al.,[46] the authors demonstrated a significantly higher *in vitro* transcorneal NT penetration from NT niosome–loaded *in situ* gel in comparison to NT marketed suspension; however, the performance of the formulation was not evaluated *in vivo*. Because surface and inner ocular tissues (such as cornea, ICB, AH, and VH) are the major sites of fungal infections and the targets for NT in antifungal therapy, the present study sought to undertake a comparative evaluation of the concentration of NT from the optimized NLCs and marketed suspension (Natacyn®) in various ocular tissues. To the best of our knowledge, this is the first study evaluating the effectiveness of NLCs in the ocular delivery of NT.

In the *in vivo* ocular biodistribution assessment, NT-PEG-NLCs were compared to their non-PEGylated counterparts and to marketed Natacyn® suspension at 5% and 0.3% (diluted marketed formulation). The comparison of NT concentrations from NT-PEG-NLC and NT-NLC in the ocular tissues was undertaken to determine the effect of PEGylation on the NT-loaded NLCs. In case of the marketed suspensions, 5% Natacyn® represented the marketed dose, whereas the 0.3% represented the dose-normalized concentration with the formulated NT-PEG-NLCs. These comparisons at the marketed and dose-normalized concentrations aided in delineating the effectiveness of the nanoparticle formulations in terms of ocular delivery of NT.

The NT-PEG-NLC exhibited significantly higher concentration (~3 folds higher) in the cornea in comparison to NT-NLC. The concentration of NT from NT-PEG-NLC was significantly higher in ICB and VH, also in comparison to the NT-NLC formulation. This observation of higher

concentrations associated with NT-PEG-NLC over the non-PEGylated counterpart is in line with the numerous literature reports that state that the PEG surface coating facilitates in the better diffusion of NLCs across the corneal epithelium and mucosal layers.[30,41,42]

The dose-normalized comparison of NT-PEG-NLC and diluted Natacyn® (0.3%) yielded a ~2-fold higher concentration of NT from NT-PEG-NLC than diluted Natacyn® (0.3%) in both cornea and ICB. The NT concentrations in AH and VH did not show any statistical difference, indicating that similar NT concentrations were obtained from NT-PEG-NLC and Natacyn® (0.3%). This *in vivo* data demonstrate that the NT-NLCs are less bioavailable than their PEGylated counterparts (both having particle size in the range of 200-250 nm) and the marketed suspension (containing NT in micronized form) at dose-normalized concentrations (0.3%). This is in contrast to the *in vitro* transcorneal permeation data (NT-PEG-NLCs > NT-NLCs > Natacyn®); however, it should be noted that the *in vitro* setup conditions are significantly different (static) from the *in vivo* environment, which is very dynamic in nature and has additional precorneal barriers such as the mucus layer. An added advantage of PEGylation is that it allows efficient penetration across mucus layers.[41,42] Thus, a larger number of NT-PEG-NLC particles will be able to reach the corneal epithelium (penetrating through the mucus layers) than the NT-NLCs that can get trapped in the mucus meshwork.[30,40-42] As a result, the NT-PEG-NLCs demonstrate greater *in vivo* ocular BA, whereas, contrary to the *in vitro* result, BA from the NT-NLCs is decreased. Thus, a combination of better penetration across the mucus as well as better transcorneal permeability of the nanoparticles leads to the overall enhanced BA from these NT-PEG-NLC formulations.

Natacyn® (5%) showed ~2-fold higher concentration in cornea than NT-PEG-NLC. This could be attributed to a 16-fold higher dose for Natacyn® (5%; the marketed dose) than NT-PEG-NLC (0.3%). It should be noted that the dose of the marketed formulation which was 16-fold higher led to only a 2-fold increase in corneal concentrations compared to the NT-PEG-NLC. In contrast, a nonsignificant difference in NT concentration levels was obtained from the NT-PEG-NLC and Natacyn® (5%) in the ICB and AH tissues, which again indicated that a 16-fold higher dose could not lead to significantly higher NT concentrations in the deeper tissues. In case of VH, a significantly higher NT concentration (~4 folds) was observed from NT-PEG-NLC in comparison to Natacyn® (5%). The observation that Natacyn® (5%) produced higher corneal NT concentrations, whereas NT-PEG-NLC delivered equivalent/higher NT concentrations in the AH, ICB, and VH tissues could be associated with the NT-PEG-NLC penetrating better across the corneal epithelium and thus into the ocular tissues in account of the strong hydrophilicity provided by the PEG coating, which aided in its faster diffusion across the corneal epithelium and mucosa.[39,40,47] In addition, the involvement of the conjunctival-scleral pathway could also be associated with the better penetration of NT-PEG-NLC formulations because the conjunctival-scleral pathway has been attributed to be an important factor in improving and enhancing the permeation of NLC systems in comparison to the conventional ocular dosage forms such as the suspensions.[17,47]

In the *in vivo* evaluation, it is also interesting to note that there was an approximately 16-fold decrease in both benzalkonium chloride and NT concentrations in the marketed formulation when 5% Natacyn® was diluted to 0.3%. However, this 16-fold decrease in the concentration gradient and possible permeation enhancer translated to only a ≈4-fold decrease in NT concentration in the cornea and a 2.5-fold decrease in NT concentrations in the iris-ciliary bodies. This indicates that for the marketed formulation, the concentration of drug in the tear fluid primarily governs the BA. It should be noted that no preservatives have been added to the NT nanoparticle formulations in this study, and when added, they can only lead to an improvement in the ocular BA (assuming no incompatibility exists).

In OFI, such as fungal keratitis, the anterior segment tissues such as cornea, ICB, and AH are majorly affected.[48] Cornea is characterized by the debridement of its epithelium, which facilitates the passage of the antifungal agents such as NT through its layers and into the inner ocular tissues.[5,48,49] However, as the healing of cornea begins during the course of antifungal therapy, the drug permeation reduces on account of restoration of the corneal epithelium integrity. Hence, this could pose as a potential risk for the relapse of the fungal infections due to subtherapeutic drug concentrations achieved in the inner layers of ICB, AH, and VH during the corneal healing process. In such a case, NT-PEG-NLC could provide an alternative approach to the conventional NT suspension by achieving similar concentrations in the inner ocular tissues of ICB, AH, and VH at a markedly reduced dose (1/16 of the marketed dose).

Conclusion

This study reports the preparation and optimization of NT-loaded surface-coated PEGylated NLC using Box-Behnken design, and to the best of our knowledge, this is the first study that reports the *in vivo* ocular biodistribution for NT from NLCs. The optimized NT-PEG-NLCs were found to have small particle size, narrow PDI, and a high NT entrapment with a minimum stability of 1 month. The NT-PEG-NLCs exhibited significantly higher transcorneal permeation and flux than the marketed suspension (Natacyn®), *in vitro*. The *in vivo* ocular biodistribution of NT-PEG-NLC indicated that the concentration of NT from Natacyn® in cornea was significantly higher than that from NT-PEG-NLC. However, it should be noted that the NT load in NT-PEG-NLC (0.3%) was 1/16 of the marketed suspension. In spite of this, NT-PEG-NLC could permeate the intact cornea to reach the ICB, AH, and VH tissues, and the difference in NT concentration obtained from NT-PEG-NLC and marketed Natacyn® (5%) suspension was statistically nonsignificant. To further evaluate the ocular suitability of the NT-PEG-NLC system, it is essential to determine its ocular safety and efficacy in fungal keratitis models, *in vivo*. Because NT-PEG-NLCs showed better penetration across intact cornea to reach the inner ocular tissues at a lower concentration, they could be a potential alternative during the ocular antifungal regimen. During the fungal keratitis therapy, when cornea is healing, it is essential for the drug to penetrate the nearly intact cornea to reach inner ocular tissues and prevent the relapse of infection. Summarizing the above investigation in determining the *in vivo* ocular biodistribution of NT from its NLC system, the NT-PEG-NLC system (at a lower NT load of 0.3%) showed increased ability to penetrate the intact cornea and to provide concentrations statistically similar to marketed suspension (at a higher dose of 5%) in the inner ocular tissues, indicating that it could be a potential alternative to the conventional marketed suspension during the course of the therapy for fungal keratitis.

Acknowledgments

This study was supported by the Graduate Student Council Research Grants Program, undertaken by the University of Mississippi and National Institute of General Medical Sciences, National Institutes of Health (Grant: P20 GM104932). The content is solely the responsibility of the authors and does not necessarily represent the official views of the National Institutes of Health.

References

1. Centers for Disease Control and Prevention. *Fungal Diseases*. Atlanta, GA: CDC; 2014. Available at: http://wwwcdcgov/fungal/diseases/indexhtml. Accessed May 9, 2018.
2. Collier S, Gronostaj M, MacGurn A, Cope J, Yoder J, Beach M. Estimated burden of keratitis—United States, 2010. *MMWR*. 2014;63:1027-1030.
3. Huang S, Dugel P, Williams G, et al. Notes from the field: multistate outbreak of postprocedural fungal endophthalmitis associated with a single compounding pharmacy—United States, March-April 2012. *MMWR*. 2012;61:310-311.
4. Jeng B, Gritz D, Kumar A, et al. Epidemiology of ulcerative keratitis in Northern California. *Arch Ophthalmol*. 2010;128(8):1022-1028.
5. Thomas P, Kaliamurthy J. Mycotic keratitis: epidemiology, diagnosis and management. *Clin Microbiol Infect*. 2013;19(3):210-220.
6. Müller G, Kara-José N, de Castro R. Antifungals in eye infections: drugs and routes of administration. *Rev Bras Oftalmol*. 2013;72(2):132-141.
7. Qiu S, Zhao G, Lin J, et al. Natamycin in the treatment of fungal keratitis: a systematic review and meta-analysis. *Int J Ophthalmol*. 2015:597-602.
8. Patil A, Majumdar S. Echinocandins in ocular therapeutics. *J Ocul Pharmacol Ther*. 2017;33(5):340-352.
9. O'Day D, Head W, Robinson R, Clanton J. Corneal penetration of topical amphotericin B and natamycin. *Curr Eye Res*. 1986;5(11):877-882.
10. Liu C, Chiu H, Wu W, Sahoo S, Hsu C. Novel lutein loaded lipid nanoparticles on porcine corneal distribution. *J Ophthalmol*. 2014;2014:11.
11. Liu D, Li J, Pan H, et al. Potential advantages of a novel chitosan-N-acetylcysteine surface modified nanostructured lipid carrier on the performance of ophthalmic delivery of curcumin. *Sci Rep*. 2016;6.
12. Battaglia L, Serpe L, Foglietta F, et al. Application of lipid nanoparticles to ocular drug delivery. *Exp Opin Drug Deliv*. 2016;13(12):1743-1757.
13. Poonia N, Kharb R, Lather V, Pandita D. Nanostructured lipid carriers: versatile oral delivery vehicle. *Future Sci OA*. 2016;2(3).
14. Farace C, Sánchez-Moreno P, Orecchioni M, et al. Immune cell impact of three differently coated lipid nanocapsules: pluronic, chitosan and polyethylene glycol. *Sci Rep*. 2016;6:18423.
15. Jiang W, Wang J, Yang L, et al. Nanostructured lipid carriers modified with PEGylated carboxymethylcellulose polymers for effective delivery of docetaxel. *RSC Adv*. 2015;5(110):90386-90395.
16. Zhang X, Gan Y, Gan L, Nie S, Pan W. PEGylated nanostructured lipid carriers loaded with 10-hydroxycamptothecin: an efficient carrier with enhanced anti-tumour effects against lung cancer. *J Pharm Pharmacol*. 2008;60(8):1077-1087.
17. Balguri S, Adelli G, Bhagav P, Repka M, Majumdar S. Development of nano structured lipid carriers of ciprofloxacin for ocular delivery: characterization, in vivo distribution and effect of PEGylation. *Invest Ophthalmol Visual Sci*. 2015;56(7), 2269-2269.
18. Thangabalan B, Kumar V. Analytical method development and validation of natamycin in eye drop by RP-HPLC. *Asian J Pharm Clin Res*. 2013;6(1):134-135.
19. Patil A, Lakhani P, Majumdar S. Current perspectives on natamycin in ocular fungal infections. *J Drug Deliv Sci Technol*. 2017;41(C):206-212.
20. Barar J, Asadi M, Mortazavi-Tabatabaei S, Omidi Y. Ocular drug delivery; impact of in vitro cell culture models. *J Ophthalmic Vis Res*. 2009;4(4):238-252.
21. McMillan J, Batrakova E, Gendelman H. Chapter 14-cell delivery of therapeutic nanoparticles. In: Antonio V, ed. *Progress in Molecular Biology and Translational Science*. Cambridge, MA: Academic Press; 2011;104:563-601.
22. Penaloza J, Marquez-Miranda V, Cabana-Brunod M, et al. Intracellular trafficking and cellular uptake mechanism of PHBV nanoparticles for targeted delivery in epithelial cell lines. *J Nanobiotechnol*. 2017;15(1):1.
23. Park J, Jeong H, Hong J, et al. The effect of silica nanoparticles on human corneal epithelial cells. *Sci Rep*. 2016;6:37762.
24. Zhou H, Hao J, Wang S, Zheng Y, Zhang W. Nanoparticles in the ocular drug delivery. *Int J Ophthalmol*. 2013;6(3):390-396.
25. Miladi K, Sfar S, Fessi H, Elaissari. Nanoprecipitation process: from particle preparation to in vivo applications. In: Vauthier C, Ponchel G, eds. *Polymer Nanoparticles for Nanomedicines: A Guide for Their Design, Preparation and Development*. Cham, Switzerland: Springer; 2017:17-55.
26. Xu Q, Kambhampati S, Kannan R. Nanotechnology approaches for ocular drug delivery. *Middle East Afr J Ophthalmol*. 2013;20(1):26-37.
27. Bhagurkar A, Repka M, Murthy S. A novel approach for the development of a nanostructured lipid Carrier formulation by hot-melt extrusion technology. *J Pharm Sci*. 2017;106(4):1085-1091.
28. Li J, Li Z, Zhou T, et al. Positively charged micelles based on a triblock copolymer demonstrate enhanced corneal penetration. *Int J Nanomedicine*. 2015;10:6027-6037.
29. Gaudana R, Ananthula H, Parenky A, Mitra A. Ocular drug delivery. *AAPS J*. 2010;12:348-360.
30. Mun E, Morrison P, Williams A, Khutoryanskiy V. On the barrier properties of the cornea: a microscopy study of the penetration of fluorescently labeled nanoparticles, polymers, and sodium fluorescein. *Mol Pharm*. 2014;11:3556-3564.
31. Siafaka P, Üstündağ Okur N, Karavas E, Bikiaris D. Surface modified multifunctional and stimuli responsive nanoparticles for drug targeting: current status and uses. *Int J Mol Sci*. 2016;17(9).
32. Azhar Shekoufeh Bahari L, Hamishehkar H. The impact of variables on particle size of solid lipid nanoparticles and nanostructured lipid carriers; a comparative literature review. *Adv Pharm Bull*. 2016;6(2):143-151.
33. Peng J, Dong W, Li L, et al. Effect of high-pressure homogenization preparation on mean globule size and large-diameter tail of oil-in-water injectable emulsions. *J Food Drug Anal*. 2015;23(4):828-835.
34. Ferreira M, Chaves L, Lima S, Reis S. Optimization of nanostructured lipid carriers loaded with methotrexate: a tool for inflammatory and cancer therapy. *Int J Pharm*. 2015;492(1−2):65-72.
35. Gupta S, Kesarla R, Chotai N, Misra A, Omri A. Systematic approach for the formulation and optimization of solid lipid nanoparticles of efavirenz by high pressure homogenization using design of experiments for brain targeting and enhanced bioavailability. *Biomed Res Int*. 2017;2017:18.
36. Üner M, Yener G. Importance of solid lipid nanoparticles (SLN) in various administration routes and future perspectives. *Int J Nanomedicine*. 2007;2(3):289-300.
37. Das S, Chaudhury A. Recent advances in lipid nanoparticle formulations with solid matrix for oral drug delivery. *AAPS PharmSciTech*. 2011;12(1):62-76.
38. Gukasyan H, Kim K, Lee V. The conjunctival barrier in ocular drug delivery. In: Ehrhardt C, Kim K-J, eds. *Drug Absorption Studies: In Situ, In Vitro and In Silico Models*. Boston, MA: Springer US; 2008:307-320.
39. Wang Y, Rajala A, Rajala R. Lipid nanoparticles for ocular gene delivery. *J Funct Biomater*. 2015;6(2):379-394.
40. De Campos A, Sánchez A, Gref R, Calvo P, Alonso M. The effect of a PEG versus a chitosan coating on the interaction of drug colloidal carriers with the ocular mucosa. *Eur J Pharm Sci*. 2003;20(1):73-81.
41. Lai S, Wang Y, Hanes J. Mucus-penetrating nanoparticles for drug and gene delivery to mucosal tissues. *Adv Drug Deliv Rev*. 2009;61(2):158-171.
42. Xu Q, Boylan N, Cai S, Miao B, Patel H, Hanes J. Scalable method to produce biodegradable nanoparticles that rapidly penetrate human mucus. *J Control Release*. 2013;170(2):279-286.
43. Balguri S, Adelli G, Janga K, Bhagav P, Majumdar S. Ocular disposition of ciprofloxacin from topical, PEGylated nanostructured lipid carriers: effect of molecular weight and density of poly (ethylene) glycol. *Int J Pharm*. 2017;529(1-2):32-43.
44. Bhatta R, Chandasana H, Chhonker Y, et al. Mucoadhesive nanoparticles for prolonged ocular delivery of natamycin: in vitro and pharmacokinetics studies. *Int J Pharm*. 2012;432(1):105-112.
45. Chandasana H, Prasad Y, Chhonker Y, et al. Corneal targeted nanoparticles for sustained natamycin delivery and their PK/PD indices: an approach to reduce dose and dosing frequency. *Int J Pharm*. 2014;477(1):317-325.
46. Paradkar M, Parmar M. Formulation development and evaluation of Natamycin niosomal in-situ gel for ophthalmic drug delivery. *J Drug Deli. Sci Technol*. 2017;39:113-122.
47. Balguri S, Adelli G, Majumdar S. Topical ophthalmic lipid nanoparticle formulations (SLN, NLC) of indomethacin for delivery to the posterior segment ocular tissues. *Eur J Pharm Biopharm*. 2016;109:224-235.
48. Thomas P. Fungal infections of the cornea. *Eye*. 2003;17(8):852-862.
49. Thomas P. Current perspectives on ophthalmic mycoses. *Clin Microbiol Rev*. 2003;16(4):730-797.